

PS and SP converted wave reflection coefficients and their application to time-lapse difference AVO

Shahin Jabbari and Kris Innanen

ABSTRACT

Multicomponent time-lapse amplitude variation with offset (AVO) may improve approximating time-lapse difference data. The difference data during the change in a reservoir from the baseline survey relative to the monitor survey are described for converted waves. We defined a framework for the difference reflection data, $\Delta R_{PS}(\theta)$, and $\Delta R_{SP}(\phi)$, in order of physical change or baseline interface contrast and time-lapse changes. A framework for linear and nonlinear time-lapse difference data are formulated using amplitude variation with offset (AVO) methods. The nonlinear higher order terms represent corrections appropriate for time-lapse problems especially for large contrasts cases. We conclude that in many plausible time-lapse scenarios the increase in accuracy associated with higher order corrections is non-negligible for converted wave. Furthermore the third order approximation terms in difference data emphasizes on the difference between exact $\Delta R_{PS}(\theta)$ and $\Delta R_{SP}(\phi)$.

INTRODUCTION

Time-lapse measurements provide a tool to monitor the dynamic changes in subsurface properties during the time of the exploitation of a reservoir. In the time-lapse monitoring process, a baseline survey is acquired prior to certain production processes of a reservoir. This is followed by one or more seismic surveys (monitor surveys) over a particular interval of time when geological/geophysical characteristics of a reservoir may change. Comparison of repeated seismic surveys over months, years, or decades adds the dimension of calendar time to the seismic data. The time-lapse difference data between the baseline and monitor surveys indicate the change in the amplitude and travel time of the seismic trace (Greaves and Fulp, 1987; Lumley, 2001; Arts et al., 2004). Time-lapse seismic captures dynamics of the reservoir which are not predicted by static reservoir modeling but is typically characterized by simulation models. Major oil companies now use time-lapse seismic in reservoir management (Johnston, 2013; Waal and Calvert, 2003; Tura, 2003). The difference data during the change in a reservoir from the baseline survey to the monitor survey can be described through applying the perturbation theory. The perturbation is presented here quantifies the changes in P wave and S wave velocities and density from the time of the baseline relative to the time of the monitor survey (Innanen et al., 2014; Stolt and Weglein, 2012).

Although P-wave seismic is the primary survey method in seismology, using multi-component recording can improve and support P-wave seismic data, especially for rocks with similar P-wave properties which may show a greater variation in S-wave properties. Multicomponent surveying has been developed rapidly in both land and marine acquisition and processing techniques, with many applications in structural imaging, lithologic estimation, anisotropy analysis, and reservoir monitoring. The elastic properties of a rock, as well as acoustic properties, change when the pressure and fluid flow is altered in a reservoir

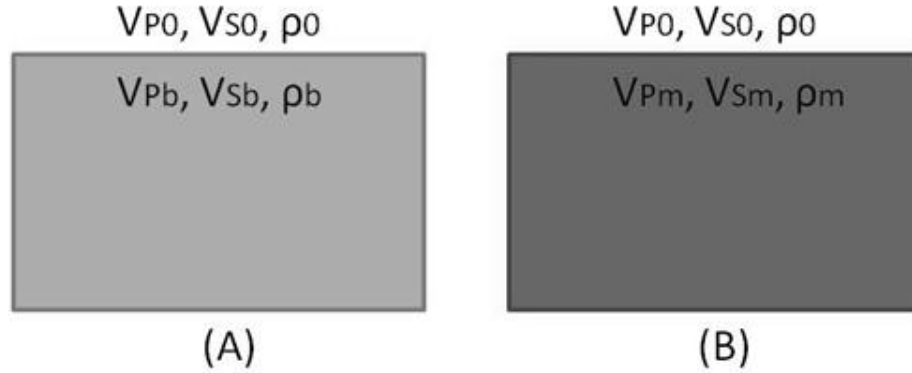


FIG. 1. Rock properties of the model at the time of the baseline(A) and monitor (B) survey.

due to production. This raise the necessity of multicomponent 4D time-lapse analysis in a reservoir (Stewart et al., 2002, 2003). Time-lapse amplitude variation with offset (time-lapse AVO) connotes the analysis of changes to the offset or angle dependence of reflection coefficients from the baseline to the monitor survey.

A framework has been formulated to model linear and nonlinear elastic time-lapse difference for P-P sections (Jabbari et al., 2015). The study described here focuses on applying linear and nonlinear time-lapse amplitude variation with offset methods to model the difference data for converted wave and more specifically to investigate the deference between SP and PS wave in nonlinearity.

Theory: Zoeppritz matrix

We will consider two seismic experiments involved in a time-lapse survey, a baseline survey followed by a monitoring survey. The P-wave and S-wave velocities and the density change from the time of the baseline survey relative to the monitoring survey (Figure 1). This pair of models is consistent with an unchanging cap rock overlying a porous target which is being produced. Let V_{P_0}, V_{S_0}, ρ_0 and V_{P_x}, V_{S_x}, ρ_x be the rock properties of the cap rock and reservoir and a P wave is impinging on the boundary of a planar interface between these two elastic media (Figure 2). Amplitudes of reflected and transmitted P and S waves are calculated through setting the boundary conditions in the Zoeppritz equations which can be rearranged in matrix form e.g. (Aki and Richards, 2002; Keys, 1989):

$$P \begin{bmatrix} R_{PP} \\ R_{PS} \\ T_{PP} \\ T_{PS} \end{bmatrix} = b_P \tag{1}$$

where

$$P \equiv \begin{bmatrix} -\sin \theta & -\sqrt{1 - B^2 \sin^2 \theta} \\ \sqrt{1 - \sin^2 \theta} & -B \sin \theta \\ 2B^2 \sin \theta \sqrt{1 - \sin^2 \theta} & B(1 - 2B^2 \sin^2 \theta) \\ -1 + 2B^2 \sin^2 \theta & 2B^2 \sin \theta \sqrt{1 - B^2 \sin^2 \theta} \end{bmatrix}$$

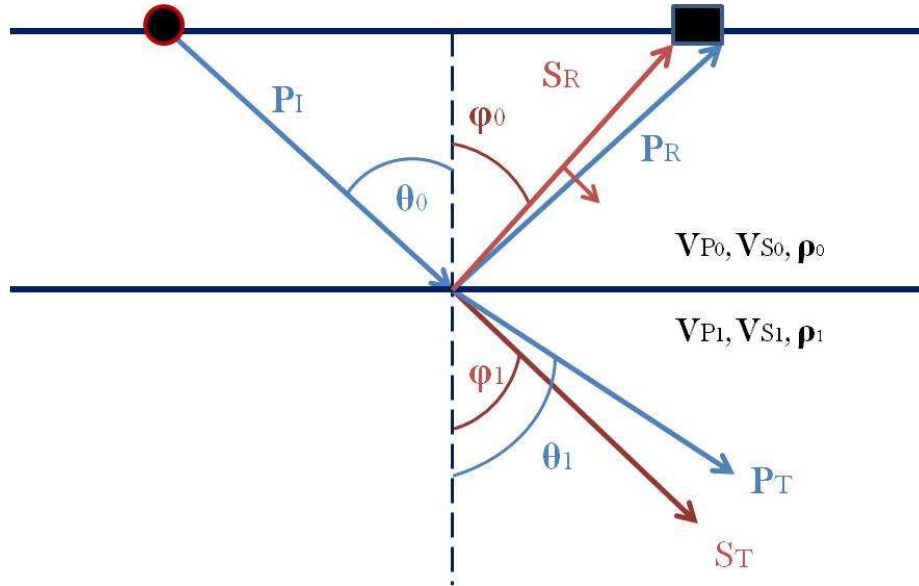


FIG. 2. Displacement amplitude of an incident P-wave with related reflected and transmitted P and S waves.

$$\begin{bmatrix} C_x \sin \theta & \sqrt{1 - D_x^2 \sin^2 \theta} \\ \sqrt{1 - C_x^2 \sin^2 \theta} & -D_x \sin \theta \\ 2A_x D_x^2 \sin \theta \sqrt{1 - C_x^2 \sin^2 \theta} & A_x D_x (1 - 2D_x^2 \sin^2 \theta) \\ A_x C_x (1 - 2D_x^2 \sin^2 \theta) & -2A_x D_x^2 \sin \theta \sqrt{1 - D_x^2 \sin^2 \theta} \end{bmatrix} \quad (2)$$

θ is the P-wave incident angle, and

$$b_P \equiv \begin{bmatrix} \frac{\sin \theta}{\sqrt{1 - \sin^2 \theta}} \\ 2B^2 \sin \theta \sqrt{1 - \sin^2 \theta} \\ 1 - 2B^2 \sin^2 \theta \end{bmatrix}.$$

The ratio of elastic parameters are defined as:

$$A_x = \frac{\rho_x}{\rho_0}, \quad B = \frac{V_{S0}}{V_{P0}}, \quad B^{-1} \equiv \frac{V_{P0}}{V_{S0}}, \quad C_x = \frac{V_{Px}}{V_{P0}}, \quad D_x = \frac{V_{Sx}}{V_{P0}}, \quad E \equiv \frac{V_{Px}}{V_{S0}}, \quad F \equiv \frac{V_{Sx}}{V_{S0}}. \quad (3)$$

To drive Zoeppritz equations for SP converted wave, we will again consider the same two seismic experiments involved in a time-lapse survey, a baseline survey followed by a monitoring survey, as in Figure 1. An S wave is impinging on the boundary of a planar interface between the two elastic media (Figure 3). Amplitudes of reflected and transmitted S waves are calculated through setting the boundary conditions in the Zoeppritz equations which can be rearranged in matrix form e.g.:

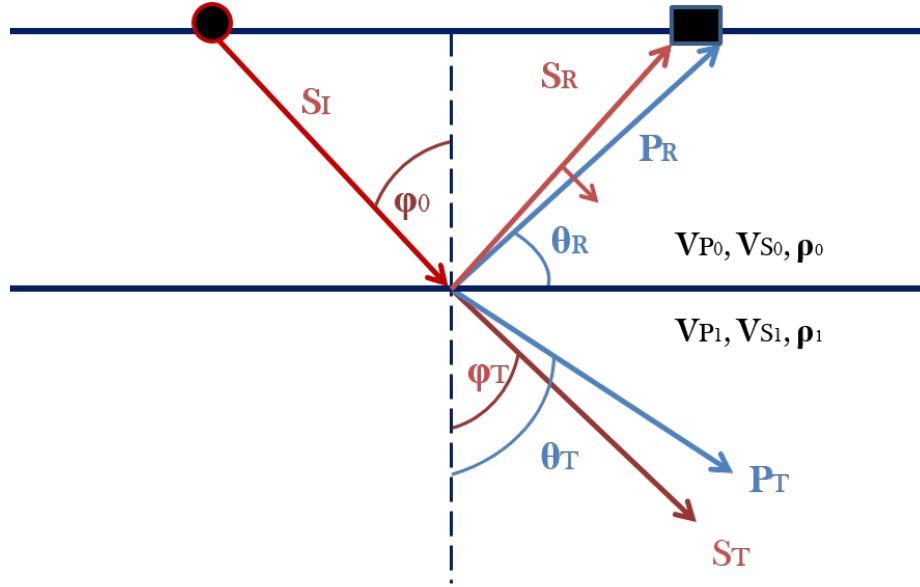


FIG. 3. Displacement amplitude of an incident S-wave with related reflected and transmitted P and S waves.

$$S \equiv \begin{bmatrix} \sin \phi & -\sqrt{1 - (B^{-1})^2 \sin^2 \phi} \\ -\sqrt{1 - \sin^2 \phi} & -B^{-1} \sin \phi \\ -2 \sin \phi \sqrt{1 - \sin^2 \phi} & B^{-1}(1 - 2 \sin^2 \phi) \\ 1 - 2 \sin^2 \phi & 2 \sin \phi \sqrt{1 - (B^{-1})^2 \sin^2 \phi} \end{bmatrix} \quad (4)$$

$$\begin{bmatrix} \frac{F_x \sin \phi}{\sqrt{1 - F_x^2 \sin^2 \phi}} & -\sqrt{1 - E_x^2 \sin^2 \phi} \\ 2A_x F_x^2 \sin \phi \sqrt{1 - F_x^2 \sin^2 \phi} & E_x \sin \phi \\ A_x F_x (1 - 2F_x^2 \sin^2 \phi) & -A_x E_x (1 - 2F_x^2 \sin^2 \phi) \\ 2A_x F_x^2 \sin \phi \sqrt{1 - E_x^2 \sin^2 \phi} & 2A_x F_x^2 \sin \phi \sqrt{1 - E_x^2 \sin^2 \phi} \end{bmatrix}$$

where ϕ is the S-wave incident angle; A_x, B^{-1}, E_x, F_x are the ratio of elastic parameters given in equation 3, and

$$c_S \equiv \begin{bmatrix} \sin \phi \\ \sqrt{1 - \sin^2 \phi} \\ 2 \sin \phi \sqrt{1 - \sin^2 \phi} \\ 1 - 2 \sin^2 \phi \end{bmatrix}.$$

Time-lapse difference data for converted wave

We calculate reflection coefficient for both types of converted waves either a reflected S wave from an incident P wave or a reflected P wave from an incident S wave. we use Matrix P in equation 2 to calculate R_{PS} and matrix S in equation 4 to calculate R_{SP} . Reflection

coefficients then, are determined by forming an auxiliary matrix P_{PS} by replacing the second columns of \mathbf{P} with b_P , and then forming another auxiliary matrix S_{SP} by replacing the second columns of \mathbf{S} with c_S :

$$R_{PS}(\theta) = \frac{\det(P_{PS})}{\det(P)} \quad R_{PS}(\phi) = \frac{\det(S_{SP})}{\det(S)}. \quad (5)$$

R_{PS} and R_{SP} for the baseline and monitor surveys are calculated using the method explained above, where rock properties for cap rock are the same, but reservoir properties change from V_{P_b} , V_{S_b} , ρ_b at the time of the baseline survey to V_{P_m} , V_{S_m} , ρ_m at the time of the monitor survey. If we replace $x = b$ for the baseline survey and $x = m$ for the monitor survey in equations 2, equation 3, and equation 4, the reflection coefficients can be calculated for both. The difference data reflection coefficient between the baseline and monitor survey is then calculated as:

$$\begin{aligned} \Delta R_{PS}(\theta) &= R_{PS}^m(\theta) - R_{PS}^b(\theta) \\ \Delta R_{SP}(\phi) &= R_{SP}^m(\phi) - R_{SP}^b(\phi). \end{aligned} \quad (6)$$

In our time-lapse study we have considered two groups of perturbation parameters. We use the same standard scattering nomenclature found in e.g. Stolt and Weglein (2012). The first group expresses the perturbation caused by propagating the wavefield from the first medium to the second medium in the baseline survey:

$$b_{VP} = 1 - \frac{V_{P_0}^2}{V_{P_b}^2}, \quad b_{VS} = 1 - \frac{V_{S_0}^2}{V_{S_b}^2}, \quad b_\rho = 1 - \frac{\rho_0}{\rho_b}. \quad (7)$$

The second group expresses the time-lapse perturbation and accounts for the changes in the monitor survey relative to the baseline survey. we define:

$$a_{VP} = 1 - \frac{V_{P_b}^2}{V_{P_m}^2}, \quad a_{VS} = 1 - \frac{V_{S_b}^2}{V_{S_m}^2}, \quad a_\rho = 1 - \frac{\rho_b}{\rho_m}. \quad (8)$$

Applying equations 7 and 8, elastic parameters in equation 3 may be re-defined in terms of perturbations in P-wave and S-wave velocities and the densities as:

$$\begin{aligned}
 A_m &= \frac{\rho_m}{\rho_0} = \frac{\rho_m}{\rho_b} \times \frac{\rho_b}{\rho_0} \\
 &= (1 - a_\rho)^{-1} \times (1 - b_\rho)^{-1}, \\
 C_m &= \frac{V_{P_m}}{V_{P_0}} = \frac{V_{P_m}}{V_{P_b}} \times \frac{V_{P_b}}{V_{P_0}} \\
 &= (1 - a_{VP})^{-\frac{1}{2}} \times (1 - b_{VP})^{-\frac{1}{2}}, \\
 D_m &= \frac{V_{S_m}}{V_{P_0}} = \frac{V_{S_m}}{V_{S_0}} \times \frac{V_{S_0}}{V_{P_0}} = \frac{V_{S_0}}{V_{P_0}} \times \frac{V_{S_m}}{V_{S_b}} \times \frac{V_{S_b}}{V_{S_0}} \\
 &= B \times (1 - a_{VS})^{-\frac{1}{2}} \times (1 - b_{VS})^{-\frac{1}{2}}, \\
 E_m &= \frac{V_{P_m}}{V_{S_0}} = \frac{V_{P_m}}{V_{P_0}} \times \frac{V_{P_0}}{V_{S_0}} = \frac{V_{P_0}}{V_{S_0}} \times \frac{V_{P_m}}{V_{P_b}} \times \frac{V_{P_b}}{V_{P_0}} \\
 &= B^{-1} \times (1 - a_{VP})^{-\frac{1}{2}} \times (1 - b_{VP})^{-\frac{1}{2}}, \\
 F_m &= \frac{V_{S_m}}{V_{S_0}} = \frac{V_{S_m}}{V_{S_b}} \times \frac{V_{S_b}}{V_{S_0}} \\
 &= (1 - a_{VS})^{-\frac{1}{2}} \times (1 - b_{VS})^{-\frac{1}{2}}.
 \end{aligned} \tag{9}$$

These parameters are substituted into Zoeppritz matrix, P, in equation 2 and Zoeppritz matrix, S, in equation 4. The elements of these new matrix now, are functions of b_ρ , b_{VP} , b_{VS} , a_ρ , a_{VP} , a_{VS} , $\sin \theta$ and $\sin \phi$. Using Taylor's series:

$$\begin{aligned}
 (1 - b_\rho)^{-1} &= 1 + b_\rho + b_\rho^2 + \dots \\
 (1 - b_{VP})^{-\frac{1}{2}} &= 1 + \frac{1}{2}b_{VP} + \frac{1 \times 3}{2 \times 4}b_{VP}^2 + \dots \\
 (1 - b_{VS})^{-\frac{1}{2}} &= 1 + \frac{1}{2}b_{VS} + \frac{1 \times 3}{2 \times 4}b_{VS}^2 + \dots \\
 (1 - a_\rho)^{-1} &= 1 + a_\rho + a_\rho^2 + \dots \\
 (1 - a_{VP})^{-\frac{1}{2}} &= 1 + \frac{1}{2}a_{VP} + \frac{1 \times 3}{2 \times 4}a_{VP}^2 + \dots \\
 (1 - a_{VS})^{-\frac{1}{2}} &= 1 + \frac{1}{2}a_{VS} + \frac{1 \times 3}{2 \times 4}a_{VS}^2 + \dots
 \end{aligned} \tag{10}$$

Zoeppritz matrix for the baseline and monitor surveys are re-calculated. The determinants and determinations in equation 5 are calculated for both surveys and the difference data reflection coefficients in equation 6 are expanded in orders of all six perturbations, $\sin^2 \theta$, and $\sin^2 \phi$:

$$\begin{aligned}
 \Delta R_{PS}(\theta) &= \Delta R_{PS}^{(1)}(\theta) + \Delta R_{PS}^{(2)}(\theta) + \Delta R_{PS}^{(3)}(\theta) + \dots \\
 \Delta R_{SP}(\phi) &= \Delta R_{SP}^{(1)}(\phi) + \Delta R_{SP}^{(2)}(\phi) + \Delta R_{SP}^{(3)}(\phi) + \dots
 \end{aligned} \tag{11}$$

The linear, second, and third order terms for time-lapse difference data for a down going

P-wave and upcoming S-wave are:

$$\begin{aligned}
\Delta R_{PS}^{(1)}(\theta) &= \left[-\frac{V_{S_0}}{V_{P_0}} \sin \theta \right] a_{VS} + \left[-\frac{1}{2} \left(2\frac{V_{S_0}}{V_{P_0}} + 1 \right) \sin \theta \right] a_\rho \\
\Delta R_{PS}^{(2)}(\theta) &= \left[-\frac{3}{4} \frac{V_{S_0}}{V_{P_0}} \sin \theta \right] a_{VS}^2 + \left[-\frac{1}{2} \sin \theta \right] a_\rho^2 + \left[\frac{1}{2} \left(2\frac{V_{S_0}}{V_{P_0}} - 1 \right) \sin \theta \right] b_\rho a_\rho \\
&\quad + \left[-\frac{1}{2} \frac{V_{S_0}}{V_{P_0}} \sin \theta \right] b_{VS} a_{VS} + \left[\frac{1}{4} \frac{V_{S_0}}{V_{P_0}} \sin \theta \right] (a_{VP} a_{VS} + a_{VP} b_{VS} + b_{VP} a_{VS}) \\
&\quad + \left[\frac{1}{8} \left(2\frac{V_{S_0}}{V_{P_0}} - 1 \right) \sin \theta \right] (a_{VP} a_\rho + b_\rho a_{VP} + a_\rho b_{VP} + a_\rho a_{VS} + a_\rho b_{VS} + b_\rho a_{VS}) \\
\Delta R_{PS}^{(3)}(\theta) &= \left[-\frac{5}{8} \frac{V_{S_0}}{V_{P_0}} \sin \theta \right] a_{VS}^3 + \left[\frac{1}{8} \left(2\frac{V_{S_0}}{V_{P_0}} - 3 \right) \sin \theta \right] a_\rho^3 + \left[-\frac{3}{8} \frac{V_{S_0}}{V_{P_0}} \sin \theta \right] \\
&\quad (b_{VS} a_{VS}^2 + b_{VS}^2 a_{VS}) + \left[\frac{1}{16} \left(6\frac{V_{S_0}}{V_{P_0}} - 1 \right) \sin \theta \right] (a_\rho^2 a_{VS} + b_\rho^2 a_{VS} + a_\rho^2 b_{VS}) + \\
&\quad \left[\frac{1}{16} \left(4\frac{V_{S_0}}{V_{P_0}} - 1 \right) \sin \theta \right] (a_\rho b_{VS}^2 + a_\rho a_{VS}^2 + b_\rho a_{VS}^2) + \left[\frac{1}{16} \left(2\frac{V_{S_0}}{V_{P_0}} - 1 \right) \right. \\
&\quad \left. \sin \theta \right] (b_\rho a_{VP}^2 + b_\rho^2 a_{VP} + a_\rho b_{VP}^2 + a_\rho^2 b_{VP} + a_\rho^2 a_{VP} + a_\rho a_{VP}^2) + \\
&\quad \left[\frac{1}{8} \frac{V_{S_0}}{V_{P_0}} \sin \theta \right] (b_{VP}^2 a_{VS} + a_{VP}^2 b_{VS} + a_{VP}^2 a_{VS} + b_{VP} b_{VS} a_{VS} + a_{VP} b_{VS} a_{VS}) \\
&\quad + \left[\frac{1}{8} \left(6\frac{V_{S_0}}{V_{P_0}} - 1 \right) \sin \theta \right] (b_\rho^2 a_\rho + b_\rho a_\rho^2) + \left[\frac{1}{32} \left(2\frac{V_{S_0}}{V_{P_0}} - 1 \right) \sin \theta \right] (a_\rho b_{VP} a_{VS} \\
&\quad + a_\rho b_{VP} b_{VS} + b_\rho a_{VP} a_{VS} + b_\rho a_{VP} b_{VS} + a_\rho a_{VP} a_{VS} + a_\rho a_{VP} b_{VS} + b_\rho b_{VP} a_{VS}) \\
&\quad \left[\frac{1}{4} \frac{V_{S_0}}{V_{P_0}} \sin \theta \right] (b_\rho b_{VS} a_{VS} + a_\rho b_{VS} a_{VS}) + \left[\frac{1}{2} \frac{V_{S_0}}{V_{P_0}} \sin \theta \right] (b_\rho a_\rho a_{VS} + b_\rho a_\rho b_{VS}) \\
&\quad + \left[\frac{3}{16} \frac{V_{S_0}}{V_{P_0}} \sin \theta \right] (a_{VP} b_{VS}^2 + a_{VP} a_{VS}^2 + b_{VP} a_{VS}^2)
\end{aligned} \tag{12}$$

The linear, second, and third order terms for time-lapse difference data for a down going

S-wave and upcoming P-wave are:

$$\begin{aligned}
 \Delta R_{SP}^{(1)}(\phi) &= \left[-\frac{V_{S_0}}{V_{P_0}} \sin \phi \right] a_{VS} + \left[-\frac{1}{2} \left(2\frac{V_{S_0}}{V_{P_0}} + 1 \right) \sin \phi \right] a_{\rho} \\
 \Delta R_{SP}^{(2)}(\phi) &= \left[-\left(\frac{3}{4} \right) \frac{V_{S_0}}{V_{P_0}} \sin \phi \right] a_{VS}^2 + \left[-\frac{1}{2} \sin \phi \right] a_{\rho}^2 + \left[\frac{1}{2} \left(2\frac{V_{S_0}}{V_{P_0}} - 1 \right) \sin \phi \right] b_{\rho} a_{\rho} \\
 &\quad + \left[-\left(\frac{1}{2} \right) \frac{V_{S_0}}{V_{P_0}} \sin \phi \right] b_{VS} a_{VS} + \left[\left(\frac{1}{4} \right) \frac{V_{S_0}}{V_{P_0}} \sin \phi \right] (a_{VP} a_{VS} + a_{VP} b_{VS} + b_{VP} a_{VS}) \\
 &\quad + \left[\frac{1}{8} \left(2\frac{V_{S_0}}{V_{P_0}} - 1 \right) \sin \phi \right] (a_{VP} a_{\rho} + b_{\rho} a_{VP} + a_{\rho} b_{VP} + a_{\rho} a_{VS} + a_{\rho} b_{VS} + b_{\rho} a_{VS}) \\
 \Delta R_{SP}^{(3)}(\phi) &= \left[\left(\frac{3}{8} \right) \frac{V_{S_0}}{V_{P_0}} \sin \phi \right] a_{VS}^3 + \left[\frac{1}{8} \left(10\frac{V_{S_0}}{V_{P_0}} + 1 \right) \sin \phi \right] (a_{\rho}^3 + b_{VS} b_{\rho} a_{VS} + b_{VS} a_{\rho} a_{VS} \\
 &\quad + b_{\rho} a_{VS}^2 + a_{\rho} a_{VS}^2 + a_{\rho} b_{VS}^2) + \left[\frac{1}{32} \left(2\frac{V_{S_0}}{V_{P_0}} - 1 \right) \sin \phi \right] (b_{VP} b_{\rho} a_{VS} + \\
 &\quad b_{VP} a_{\rho} a_{VS} + b_{VS} b_{\rho} a_{VP} + b_{VS} a_{\rho} a_{VP} + b_{VP} a_{\rho} b_{VS} + a_{VP} b_{\rho} a_{VS} + a_{VP} a_{\rho} a_{VS}) \\
 &\quad + \left[\frac{1}{4} \left(6\frac{V_{S_0}}{V_{P_0}} + 1 \right) \sin \phi \right] (a_{\rho} b_{\rho} a_{VS} + a_{\rho} b_{\rho} b_{VS}) + \left[\frac{1}{16} \left(22\frac{V_{S_0}}{V_{P_0}} + 3 \right) \sin \phi \right] \\
 &\quad (a_{VS} a_{\rho}^2 + b_{VS} a_{\rho}^2 + a_{VS} b_{\rho}^2) + \left[\frac{1}{8} \left(14\frac{V_{S_0}}{V_{P_0}} + 3 \right) \sin \phi \right] (b_{\rho} a_{\rho}^2 + a_{\rho} b_{\rho}^2) \left[\frac{1}{16} + \right. \\
 &\quad \left. \left(2\frac{V_{S_0}}{V_{P_0}} - 1 \right) \sin \phi \right] (b_{VP} a_{\rho}^2 + a_{VP} b_{\rho}^2 + a_{VP} a_{\rho}^2 + a_{VP}^2 b_{\rho} + a_{VP}^2 a_{\rho} + b_{VP}^2 a_{\rho}) \\
 &\quad + \left[\left(\frac{5}{8} \right) \frac{V_{S_0}}{V_{P_0}} \sin \phi \right] (a_{VS} b_{VS}^2 + b_{VS} a_{VS}^2) + \left[\left(\frac{1}{8} \right) \frac{V_{S_0}}{V_{P_0}} \sin \phi \right] (a_{VS} b_{VP}^2 + b_{VS} a_{VP}^2 \\
 &\quad + a_{VS} a_{VP}^2 + a_{VS} b_{VS} a_{VP} + a_{VS} b_{VS} b_{VP}) + \left[\left(\frac{3}{16} \right) \frac{V_{S_0}}{V_{P_0}} \sin \phi \right] \\
 &\quad (b_{VP} a_{VS}^2 + a_{VP} b_{VS}^2 + a_{VP} a_{VS}^2)
 \end{aligned} \tag{13}$$

Investigating equation 12 and equation 13 shows that third order term in ΔR_{SP} and ΔR_{SP} are different. This difference emphasizes that, the difference between PS and SP reflection coefficient can be verified by higher order approximations as the linear and second order terms are identical in equation 12 and equation 13.

Numerical examples for converted wave

In this section, we examine the derived linear and nonlinear difference time-lapse AVO terms for PS converted wave and SP converted wave qualitatively with numerical examples. In the first example, the data used by Landrø (2001) are applied. Typical values for P-wave and S-wave velocities and density for the cap rock and reservoir (preproduction and post production), which are taken from Gullfaks 4D project, are used. In the Gullfaks field, there are +13 %, -2 %, and +4 % changes in the reservoir in P-wave and S-wave velocities and density respectively due to the production.

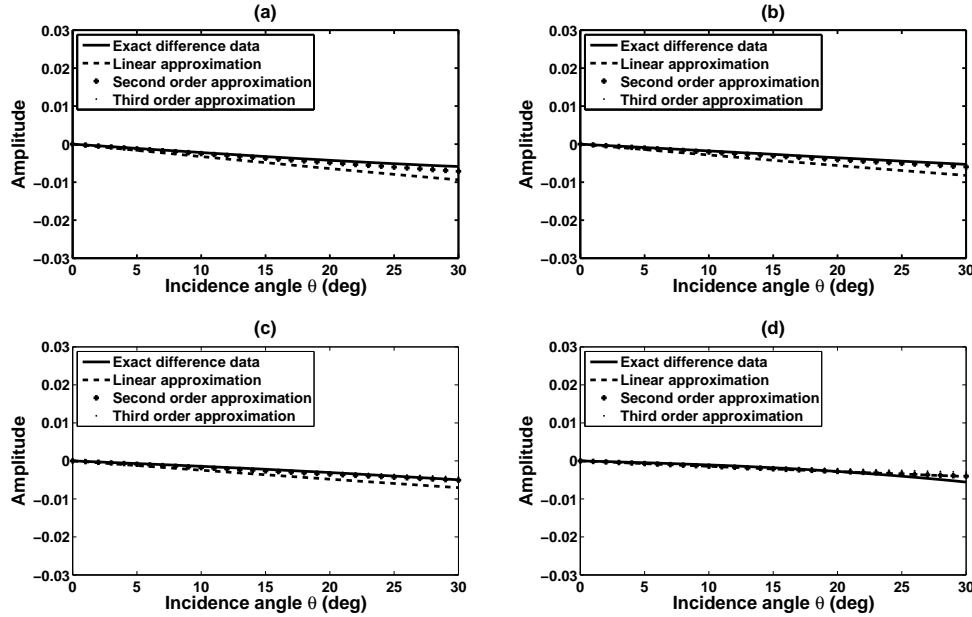


FIG. 4. ΔR_{PS} for the exact (Solid line), linear (- - -), second order (+++), and third order approximation (...).

Elastic incidence parameters: $V_{P0} = 1900m/s$, $V_{S0} = 995m/s$ and $\rho_0 = 1.95g/cc$; Baseline parameters: $V_{PBL} = 2066m/s$, $V_{SBL} = 1075m/s$ and $\rho_{BL} = 2.1300g/cc$.

a: +13 %, -2 %, and +4 %, b: +16 %, -3 %, and +5 %, c: +20 %, -4 %, and +6 %, d: +25 %, -6 %, and +8 % changes in P-wave and S-wave velocities and density respectively in the reservoir after production.

The exact difference data are compared with the calculated linear and higher order approximations in Figure 4. Results are also compared for the higher contrast in seismic parameters in the reservoir after the production. The second and third order approximations are in better agreement with the exact difference data, especially for angles below the critical angle which correspond to the range of study in this study.

The reflection coefficient for reflected P-wave due to an incident S-wave is usually different from the reflection coefficient for reflected S-wave due to an incident P-wave. The theoretical results for the first, second, and third order approximation for SP converted wave are compared with the exact difference data for the same dataset used by (Landrø,2001) in Figure 5.

For the second example, we used data by Veire (2006). Veire used two synthetic models for the reservoir: a baseline scenario with a water saturation of 10 % and an effective pressure of 2 MPa . In the monitor survey, the water saturation and effective pressure are 50 % and 8 MPa respectively. These changes altered the seismic parameters and caused 15 %, 11 %, and 1 % increase respectively in P-wave and S-wave velocities and density (Figure 4.3.b). We examined our formulation and compared them with the exact difference data not only for these changes, but also for higher contrasts (Figure 6). The theoretical results for SP converted wave are examined for the same dataset by Veire (2006) in Figure 6.

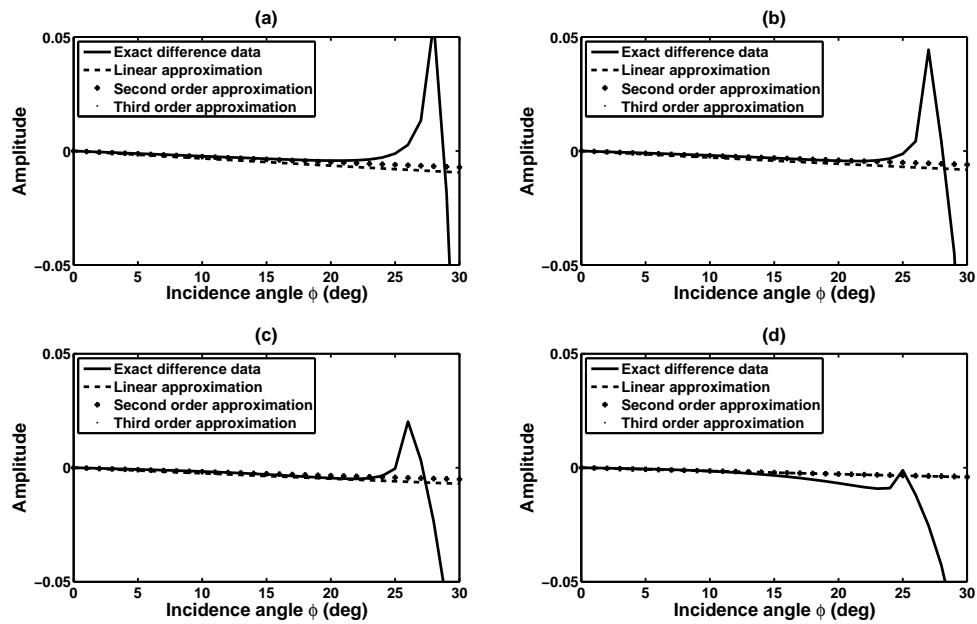


FIG. 5. ΔR_{SP} for the exact (Solid line), linear (- - -), second order (+++), and third order approximation (...).

Elastic parameters as in Figure 4.

a: +13 %, -2 %, and +4 %, b: +16 %, -3 %, and +5 %, c: +20 %, -4 %, and +6 %, d: +25 %, -6 %, and +8 % changes in P-wave and S-wave velocities and density respectively in the reservoir after production.

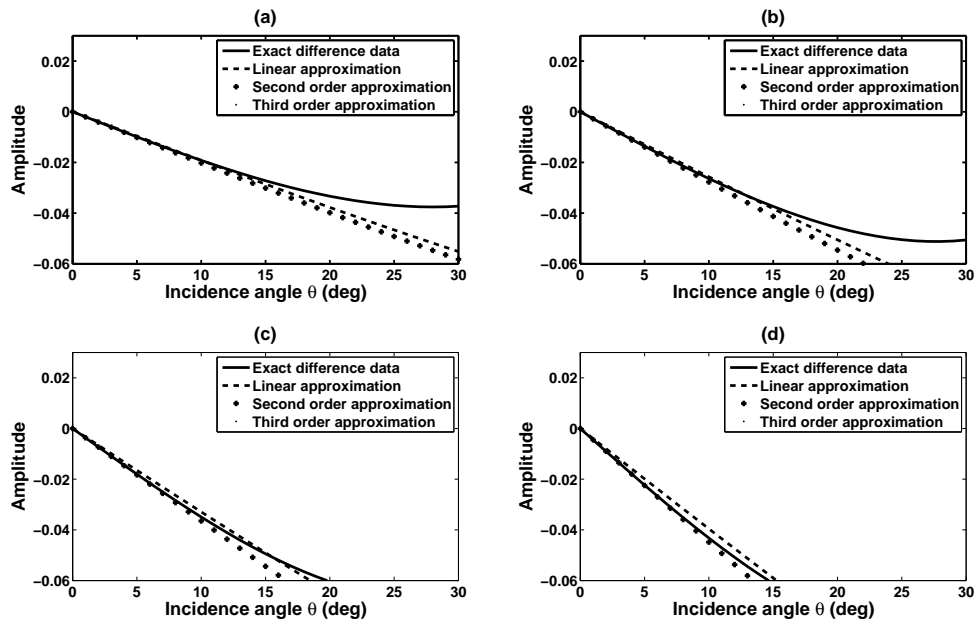


FIG. 6. ΔR_{PS} for the exact (Solid line), linear (- - -), second order (+++), and third order approximation (...).

Elastic parameters: Elastic parameters: $V_{P0} = 2000m/s$, $V_{S0} = 1000m/s$ and $\rho_0 = 2.000g/cc$;
 Baseline parameters: $V_{PBL} = 1900m/s$, $V_{SBL} = 1100m/s$ and $\rho_{BL} = 1.950g/cc$; and b. Data used by (Veire, 2006).

a: +15 %, +11 %, and +1 %, b: +20 %, +15 %, and +2 %, c: +25 %, +20 %, and +3 %, d: +30 %, +25 %, and +4 % changes in P- and S-wave velocities and density respectively in the reservoir after production.

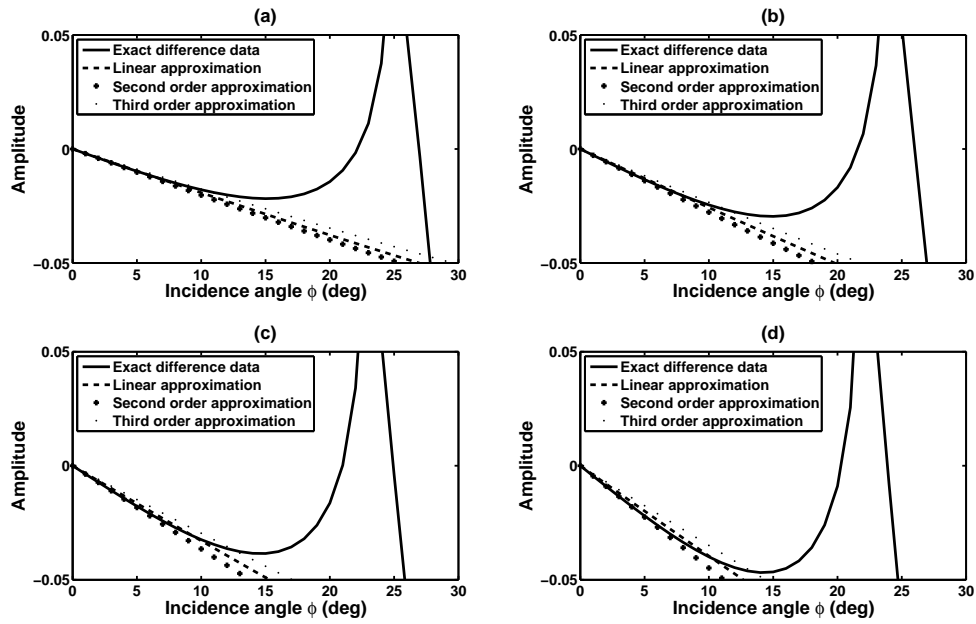


FIG. 7. ΔR_{SP} for the exact (Solid line), linear (- - -), second order (+++), and third order approximation (...).

Elastic parameters as in Figure 6.

a: +15 %, +11 %, and +1 %, b: +20 %, +15 %, and +2 %, c: +25 %, +20 %, and +3 %, d: +30 %, +25 %, and +4 % changes in P- and S-wave velocities and density respectively in the reservoir after production.

The second and third order time-lapse AVO approximations are always in better agreement with the exact difference data, especially for higher contrasts in seismic parameters. More importantly the third order approximation emphasizes on the difference between ΔR_{PS} and ΔR_{SP} by following the same trend as the exact difference in each case as in Figure 4-7.

CONCLUSIONS

Time-lapse measurements provide a tool to monitor the dynamic changes in subsurface properties during the time of the exploitation of a reservoir. Changes in the fluid saturation and pressure will have an impact in elastic parameters of subsurface, such as P wave and S wave velocities and density, which can be approximated by applying time-lapse AVO analysis methods. A well-developed AVO regimes analysis converted wave and shear waves AVO as well the P-wave AVO. Jabbari and Innanen have already investigated P-wave time-lapse AVO and showed that adding the higher order terms in ΔR_{PP} to the linear approximation for difference time-lapse data increases the accuracy of the ΔR_{PP} and corrects the error due to linearizing ΔR_{PP} (Jabbari et al., 2015). This framework was extended by formulating a framework for the difference reflection data in ΔR_{SS} , ΔR_{PS} , and ΔR_{SP} (Jabbari and Innanen, 2014, 2015). In this study we focused on the difference between ΔR_{PS} and ΔR_{SP} for SP and PS converted wave. The results showed that, including higher order terms in ΔR for converted wave improves the accuracy of approximating time-lapse difference reflection data, particularly for large contrast cases. Comparing linear, second, and third order terms for ΔR_{PS} and ΔR_{SP} indicates as we are moving toward higher order approximations; ΔR_{PS} and ΔR_{SP} are different. This confirms the difference between exact ΔR_{PS} and ΔR_{SP} which does not show up in the linear approximation case.

ACKNOWLEDGMENTS

The authors thank the sponsors of CREWES for continued support. This work was funded by CREWES industrial sponsors and NSERC (Natural Science and Engineering Research Council of Canada) through the grant CRDPJ 461179-13. Author 1 was also supported by a scholarship from the SEG Foundation.

REFERENCES

- Aki, K., and Richards, P. G., 2002, *Quantitative Seismology*: University Science Books, 2 edn.
- Arts, R., Eiken, O., Chadwick, A., Zweigel, P., van der Meer, L., and Zinszner, B., 2004, Monitoring of CO₂ injected at Sleipner using time-lapse seismic data: *Energy*, **29**.
- Greaves, R. J., and Fulp, T. J., 1987, Three-dimensional seismic monitoring of an enhanced oil recovery process: *Geophysics*, **52**, 1175–1187.
- Innanen, K. A., Naghizadeh, M., and Kaplan, S. T., 2014, Perturbation methods for two special cases of the time-lapse seismic inverse problem: *Geophysical Prospecting*, **62**, 453–474.
- Jabbari, S., and Innanen, K. A., 2014, A framework for linear and nonlinear converted wave time-lapse difference AVO: CSEG GeoConvention.
- Jabbari, S., and Innanen, K. A., 2015, A theoretical analysis of linear and nonlinear shear wave time-lapse difference AVO: CSEG GeoConvention.

- Jabbari, S., Wong, J., and Innanen, K. A., 2015, A theoretical and physical modeling analysis of the coupling between baseline elastic properties and time-lapse changes in determining difference amplitude variation with offset: *Geophysics*, **80**, No. 6, 50–53.
- Johnston, D. H., 2013, Practical application of time-lapse seismic data, *in* 2013 distinguished instructor short course, SEG.
- Keys, R. G., 1989, Polarity reversals in reflections from layered media: *Geophysics*, **54**, 900–905.
- Lumley, D. E., 2001, Time-lapse seismic reservoir monitoring: *Geophysics*, **66**, 50–53.
- Stewart, R. R., Gaiser, J., Brown, R. J., and Lawton, D. C., 2002, Tutorial: converted-wave seismic exploration: methods: *Geophysics*, **67**, No. 5, 1348–1363.
- Stewart, R. R., Gaiser, J., Brown, R. J., and Lawton, D. C., 2003, Tutorial: converted-wave seismic exploration: Application: *Geophysics*, **68**, No. 1, 40–57.
- Stolt, R. H., and Weglein, A. B., 2012, *Seismic Imaging and Inversion: Volume 1: Application of Linear Inverse Theory*: Cambridge University Press.
- Tura, A., 2003, Time-lapse seismic: Are we there yet?: *SEG Technical Program Expanded Abstracts*, 2395–2398.
- Waal, H. D., and Calvert, R., 2003, Overview of global 4d seismic implementation strategy: *Petroleum Geoscience*, **9**, 1–6.